Industrial Crops and Products 60 (2014) 326–334

Contents lists available at ScienceDirect

Industrial Crops and Products

journal homepage: www.elsevier.com/locate/indcrop

Assessment of UV exposure and aerobic biodegradation of poly(butylene adipate-*co*-terephthalate)/starch blend films coated with radiation-curable print inks containing degradation-promoting additives

Marcelo A.G. Bardi[a,b,*], Mara M.L. Munhoz[a], Rafael A. Auras[b], Luci D.B. Machado[a]

[a] Instituto de Pesquisas Energéticas e Nucleares (IPEN/CNEN-SP), Universidade de São Paulo (USP), Avenida Professor Lineu Prestes, 2242, Cidade Universitária, São Paulo, SP 05508-000, Brazil
[b] School of Packaging, Michigan State University (MSU), 448 Wilson Road, East Lansing, MI 48824, USA

ARTICLE INFO

Article history:
Received 3 February 2014
Received in revised form 7 June 2014
Accepted 20 June 2014
Available online 11 July 2014

Keywords:
PBAT
TPS
UV/EB technology
Pro-degrading additive
Composting

ABSTRACT

Biodegradable poly(butylene adipate-*co*-terephthalate) (PBAT) and thermoplastic starch (TPS) blend films were printed with white, yellow, red, blue, and black inks based on epoxy acrylate resin. Clear PBAT/TPS films were used as the control. Ink formulations were also modified with (1% w/w) and without the degradation-promoting additives cobalt stearate (CoSt) or cerium stearate (CeSt). Printed PBAT/TPS films were cured under ultraviolet light emitted by a medium-pressure mercury lamp at 10.3 kW m^{-2}, and then further aged in a accelerated weathering chamber at a total irradiance of 0.89 W m^{-2} continuously for 250 h at 50 ± 3 °C. Subsequently, samples were exposed to an aerobic composting biodegradation process at 58 °C and 55% relative humidity for 60 d. Color (L^*, a^* and b^*), gloss and hardness indexes, as well as FTIR spectra, were obtained. Thermal properties and molecular structure were monitored before and after UV exposure and biodegradation tests. The addition of CoSt affected the color, gloss and hardness of the samples exposed to UV aging. The degradation of the PBAT/TPS + CoSt films depended on the nature of the ink pigment and on their capacity to absorb UV photons. UV exposure of PBAT/TPCS samples resulted in a larger reduction of weight average molecular weight ($\bar{M}_w$) and the evolution of CO_2. The incorporation of the degradation-promoting additives increased the sensitivity of the films to UV degradation, and CoSt had a large impact in the final $\bar{M}_w$ of the samples.

1. Introduction

The large consumption and waste of short lifetime plastics have increased the environmental concerns raised by both consumers and governments over the last 5 decades (Al-Salem et al., 2009; Hopewell et al., 2009; Kijchavengkul and Auras, 2008; Thompson et al., 2009). One of the main concerns is centered on the difficulty of recycling and/or recovering contaminated plastics, which mostly end up in landfills. Hence, biotic degradation of polymers has been suggested as a tentative method for reducing polymer waste at end of life (EoL). However, the most commonly used polymers, namely the polyolefins including low, high and linear low density polyethylene (LDPE, HDPE, LLDPE) and polypropylene (PP), and poly(ethylene terephthalate) (PET) (Al-Salem et al., 2009), are largely not susceptible to biological degradation (Kijchavengkul and Auras, 2008). The collection rate of these polymers in many developing and developed countries is very low, and so they accumulate in the environment contaminating vital natural resources, including terrestrial, freshwater and marine habitats (Thompson et al., 2009).

Polyolefins and PET alternatives have been researched in an effort to replace them with biodegradable and compostable polymers. These new classes of materials can be divided into polymers derived from renewable resources, such as starch-based or cellulose-based materials, or non-renewable resources derived from petroleum, such as poly(ε-caprolactone) (PCL) or poly(butylene adipate-*co*-terephthalate) (PBAT) (Fig. 1a) (Kijchavengkul and Auras, 2008; Thompson et al., 2009). These new

* Corresponding author at: Instituto de Pesquisas Energéticas e Nucleares (IPEN/CNEN-SP), Avenida Professor Lineu Prestes, 2242, Cidade Universitária, São Paulo, SP 05508-000, Brazil. Tel.: +55 11998191633.
E-mail addresses: Marcelo.bardi@usp.br, magbardi@ipen.br (M.A.G. Bardi), mlmunhoz@ipen.br (M.M.L. Munhoz), aurasraf@msu.edu (R.A. Auras), lmachado@ipen.br (L.D.B. Machado).

http://dx.doi.org/10.1016/j.indcrop.2014.06.042
0926-6690/

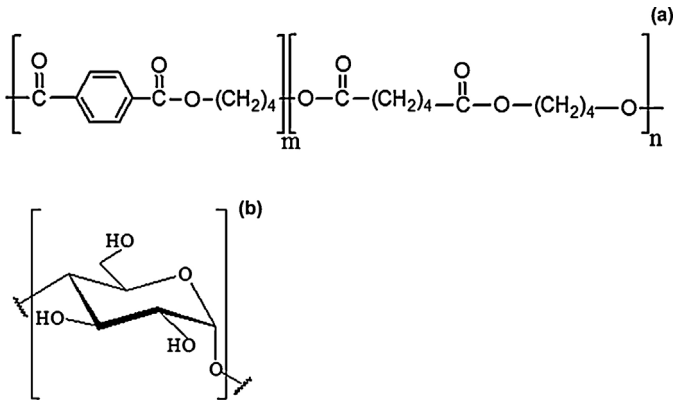

Fig. 1. Chemical structure for (a) poly(butylene adipate-*co*-terephthalate) (PBAT), and (b) starch.

polymers are easily biodegraded and bioassimilated when disposed on sites containing microorganisms capable of metabolizing their basic chemical structures (Kijchavengkul and Auras, 2008). However, in many cases these biodegradable homopolymers do not meet the physical, mechanical and thermal properties needed for industrial applications. Polymer blends, such as PBAT (Fig. 1a) and thermoplastic starch (TPS) (Fig. 1b) blends, are being developed to meet these requirements (Ojeda, 2013). To be certified as compostable, in accordance with ASTM D6400 and EN 13452, polymers must meet specific disintegration, biodegradation and ecotoxicity requirements (Briassoulis et al., 2010).

In recent years, catalytic agents have been incorporated in polymers to enhance their response to abiotic factors such as levels of UV light exposure, oxygen and temperature (Hopewell et al., 2009). The overall intention of this practice is to reduce the weight average molecular number ($\bar{M}_n$) of the polymers before exposure to biotic environments so that microorganisms can easily digest lower $\bar{M}_n$ fragments. These degradation-promoting additives are generally called pro-degrading agents, and are mainly transition metal salts. The kinetic reaction mechanism for polyolefin with such additives has been reported (Ojeda, 2013), but it is not yet completely understood for other polymers. On the another side, little is known about the timescale, extent or consequences of their degradation in natural environments (Thompson et al., 2009). ASTM D6954-04 provides some recommendations for testing polyolefin.

Ink layers applied over short lifetime plastic packaging, at around 1–10 μm in thickness after the drying/curing process, have various functions: making the product more attractive to the consumer, supplying information about the product contents, and also offering protection against physical and chemical agents. Inks are basically composed of a resin matrix, diluents, pigments, additives and a curing agent. For this kind of coating, there has been a significant increase in the application of curing induced by UV light or electron beam radiation, also called UV/EB technology. In this technology, the diluent is replaced by reactive monomers, and the formulation is converted into a high cross-linked coating film by means of free radicals generated by the incident radiation. Specifically to the UV curing process, a photoinitiator component is needed (Roy et al., 2010). Once the solid film is obtained, the cross-linked network cannot be easily undone, offering considerably high chemical and physical resistance and stability (Roy et al., 2010).

Thus, the goal of this work was to study the influence of different color inks printed on PBAT/TPS films, cured by UV-B light, and exposed to UV-A degradation followed by an aerobic biodegradation process. The effect of adding a pro-degrading additive into the ink formulation was evaluated for films exposed to UV-aging treatment and biodegradation tests.

2. Materials and methods

2.1. Materials

PBAT/TPS blend films were kindly supplied by Corn Products do Brasil (Jundiaí, SP, Brazil), and it was used as the polymeric substrate for printing the ink formulations as specified. PBAT/TPS contained no more than 50% renewable polymer (starch). The detailed formulation and production techniques are proprietary information.

The following materials were applied in preparation of the UV-curable clear formulation: Bisphenol A epoxy diacrylate (EBECRYL® 3720-TP25, Cytec Industries Inc.) diluted 25% by weight with tripropylene glycol diacrylate (TRPGDA, Cytec Industries Inc.); trimethylolpropane triacrylate (TMPTA, Cytec Industries Inc.); a 4.5/3.5/2.0 (w/w/w) blend of photoinitiators (1-hydroxycyclohexyl phenyl ketone (Irgacure 184, Ciba-Geigy Co.)/2-hydroxy-2-methyl-1-[4-(1-methylvinyl) phenyl] propanone (Esacure KIP 150, Lamberti Co.)/2-dimethylamino-2-(4-methyl-benzyl)-1-(4-morpholin-4-yl-phenyl)-butan-1-one (Irgacure 379, Ciba Specialty Chemicals Inc.), respectively; talc (Nicron® 674, Luzenac America, Inc.); polydimethylsiloxane (Pure Silicone Fluid 100,000cSt, Clearco Products Co., Inc.); quinone derivative in propoxylated glycerol tri-acrylate (Irgastab® UV 22, Ciba Specialty Chemicals Inc.); and polyethylene/polytetrafluoroethylene wax (CeraSPERSE® 164, Shamrock Technology, Inc.).

Pigments were added to the clear coating to obtain colored print inks as follows: carbon black (Printex® 45 powder, Evonik Degussa GmbH); yellow pigment derived from diarylide m-xylidide (Irgalite® Yellow LBIW, Ciba Specialty Chemicals Inc.); blue pigment derived from phtalocyanine (Hostaperm Blue B2G 01-BR, Clariant Pigmentos e Aditivos Ltda.); ruby pigment derived from monoazo (Rubide 4B, Hongyan Pigment Chemical Co., Ltd.); and titanium dioxide (Kemira® 660 RDI-S, Kemira Pigments Oy). The ratio of pigment/clear coating for the yellow, ruby and blue pigments was kept constant (21/79, w/w) to investigate only the influence of each pigment under UV curing and UV aging. Table 1 provides the nominal composition of the tested samples.

To study the effect of pro-degrading additives on the inks, 1 wt% cobalt stearate (CoSt) or 1 wt% cerium stearate (CeSt), both supplied by Strem Chemicals Inc. (Newburyport, MA, USA), was added to the ink formulation.

The samples were labeled as follows: [*BA,AA*]-*color* {*+CoSt, +CeSt*}. In this format *BA* and *AA* stand for "Before UV Aging" and "After UV Aging," respectively; *color* is the visual color as presented in Table 1; and *+CoSt* or *+CeSt* indicates the presence of cobalt stearate or cerium stearate, respectively. For example, the sample labeled as *BA-Yellow + CoSt* refers to the PBAT/TPS film coated with yellow ink containing *CoSt* before UV aging.

3. Methods

3.1. Ink layer application and curing

A manual applicator type QuickPeek® (Boanitec Indústria e Comércio Ltda., Cotia, SP, Brazil) was used to apply the colored print inks over the PBAT/TPS films. The thickness of the coating layer was 7.0 ± 1.3 μm before curing.

The coating formulations were cured at room temperature using a Labcure UV tunnel (Germetec UV and IR Technology Ltd., Rio de Janeiro, RJ, Brazil). Briefly, this equipment consists of a medium-pressure mercury lamp (main photon emission range from 320 nm to 400 nm) and a conveyor belt with adjustable speed. The UV radiation doses were measured with an EIT UV PowerPuck® radiometer (EIT Inc., Sterling, VA, USA).

Table 1
Nominal sample composition of print inks labeled accordingly to their visual color.

Component	Print ink composition (wt%)					
	Yellow	Red	Blue	Black	White	Clear
Epoxy acrylate resin	54	54	54	56	39.7	75
TMPTA monomer	10	10	10	10	–	14
Talc	3	3	3	3	–	–
Silicone	1	1	1	1	–	–
UV stabilizer	1	1	1	1	0.3	–
Photo-initiator blend	8	8	8	9	8	11
PE wax	1	1	1	1	1	–
PTFE wx	1	1	1	1	1	–
Yellow pigment	21				–	–
Ruby pigment		21		2	–	–
Blue pigment			21	3	–	–
White pigment					50	–
Carbon black				13	–	–
Total	100	100	100	100	100	100

The coated plastic films were placed on a conveyor belt that could move under the UV light beam. The power of the lamp was fixed at 11.8 kW m^{-1}, and the precise control of conveyor speed determined the radiation dose absorbed by the samples. A UV radiation dose of 5.20 kJ m^{-2} was applied to the samples at 23 °C and 45% RH.

3.2. Sample aging

The accelerated aging was performed using a QUV chamber model EQUV from Equilam Ind. e Com. Ltda. (Diadema, SP, Brazil) in accordance with ASTM D5208-09, cycle C. Fluorescent UV light bulbs with 0.89 W m^{-2} nm^{-1} irradiance (at 340 nm) were used for continuous 250-h cycles of irradiation under a UV-incident beam at 90° and at a constant temperature of 50 ± 3 °C. After exposure, aged and non-aged samples were characterized and evaluated.

3.3. Sample characterization

Color and gloss measurements were obtained using a Spectro-Guide Sphere Gloss from Byk-Gardner GmbH (Geretsried, Germany). A D65/10° geometry was used, and data collection was performed for three different positions of the samples. The $L^*a^*b^*$ coordinates and gloss index are reported for three different positions and two different samples. L^* values indicate lightness (the higher the value, the lighter the color); positive or negative a^* values indicate a reddish or greener color sample, respectively; and positive or negative b^* values indicate a yellowish and bluish color sample, respectively.

The König hardness of the films was evaluated according to ISO 1522:2006(E) using a pendulum hardness tester (Byk-Gardner GmbH, Geretsried, Germany) and is reported in seconds.

Thermal analysis was conducted with a differential scanning calorimeter (DSC) from TA Instruments, Inc., (New Castle, DE, USA) model Q50 under a dynamic atmosphere of nitrogen (flow rate: 70 mL min^{-1}). Samples around 5 mg were exposed to temperature cycles consisting of heating from room temperature to 200 °C at 20 °C min^{-1}, cooling down to −80 °C at a cooling rate of 20 °C min^{-1}, and reheating up to 200 °C. All of the DSC experiments were done in duplicate. Data for melting temperature (T_m), crystallization temperature (T_c) and glass transition (T_g) were recorded and are reported.

Each sample of UV-aged PBAT/TPS blend, control and coated, was dissolved in tetrahydrofuran (THF) (Sigma Aldrich) at 25 °C for 7 days, and then filtered through a 0.2-μm polytetrafluoroethylene (PTFE) syringe filter. Molecular weights were measured by gel permeation chromatography (GPC) with a Waters gel permeation chromatograph (Milford, MA, USA) equipped with a series of three columns (HR2, HR3, and HR4), and a Waters 2414 refractive index detector interface with Waters Breeze software from Waters Inc. (Milford, MA), using a flow rate of 1.0 mL min^{-1}, an average runtime of 45 min, and a temperature of 35 °C. The number–average and weight-average molecular weights, $\bar{M}_n$ and $\bar{M}_w$ respectively, were calculated using a calibration curve obtained from polystyrene standards (Polystyrene Shodex STD KIT SM 105, Showa Denko, Japan) with molecular weight in the range of 1.20–3.64 kDa. A third-order polynomial calibration curve was used. The $\bar{M}_n$ and $\bar{M}_w$ of the PBAT part of the blends are reported.

3.4. Biodegradation test under composting conditions

An in-house built direct-measurement respirometric system (DMR) made by bioreactors connected to a CO_2 infrared gas analyzer was used to determine the biodegradation in organic compost. Three groups of bioreactors were used: the first group of vessels contained 400 g compost (wet basis) as a control sample; the second group contained a mixture of 400 g compost (wet basis) and 8 g cellulose powder (20-μm grade, Sigma Aldrich) as a positive control; and the third group contained 400 g compost (wet basis) and 8 g of BA-PBAT/TPS, AA-PBAT/TPS, AA-*Black*, AA-*Black*-CoSt, AA-*Yellow*, or AA-*Yellow* + CoSt films cut into 1 cm × 1 cm pieces. Each sample was run in triplicate. Details of the apparatus and testing conditions can be found elsewhere (Kijchavengkul et al., 2006). The test was conducted according to ASTM D5338-11. The bioreactors were incubated in an environmental chamber at 58 ± 2 °C and 55% RH for 60 days. The compost humidity was measured every 3 days. The CO_2 evolution was continuously monitored. The percent mineralization was calculated using Eq. (1):

$$\%\text{Mineralization} = \frac{sCO_2 - bCO_2}{W \times \frac{\%C}{100} \times \frac{44}{12}} \times 100 \quad (1)$$

where sCO_2 is the amount of CO_2 from the sample or the cellulose reactor; bCO_2 is the amount of CO_2 from the compost reactor; W is the weight of sample or cellulose; and $\%C$ is the % carbon in the film sample or cellulose obtained from elemental analyses carried out on a Perkin-Elmer 2400 CHN (Waltham, MA, USA). The test met the ASTM D5338-11 requirements by producing 50.8 ± 4.0 mg of CO_2 per gram of volatile solids over the first 10 days of the test. The compost had an ash content of less than 70% and the pH was 7.9 ± 1.0. The total dry solids were quantified as 52.8%.

3.5. Ecotoxicity

After the biodegradation tests under composting conditions were complete, the content of each replicate vessel was carefully removed and thoroughly mixed. Compost (5 mg) was held in a moisture analyzer model MX50 (San Jose, CA, USA) at 105 °C until a 0.05% weight loss rate was reached, and the weight was recorded as the moisture content. The dry compost was then mixed with distilled water (1:5) and allowed to rest for 30 min prior to measuring the pH with an Omega PHB212 pH meter (Stamford, CT, USA).

The following tests were conducted in accordance with ASTM D6954-04 and OECD/OCDE 208 (2006) to evaluate plant germination and growth in the composted materials.

3.5.1. Plant germination

Compost (5 mg) was rinsed with 25 mL of distilled water and filtered. The supernatant was used as germination medium for five cress (*Lepidium sativum*) seeds placed on a Petri dish containing wet cotton, and covered by a wet filter paper and aluminum foil. Water was used as a control for the seeds. Four replicates from each sample were held at 23 ± 3 °C in the absence of light for 4 days. The percentage of germinated seeds was determined after 4 days and compared to the water control.

3.5.2. Plant growth

Compost containing the original samples exposed to the DMR was mixed (1:1) with potting soil (Sure Mix™, Michigan Grower Products, Inc., Galesburg, MI, USA). A mixture of compost used in the DMR experiment with potting soil was used as control. One *dicotyledonae* species (*Cucumis sativus*) and one *monocotyledonae* species (*Avena sativa*) were used for plant growth tests. Five replicates were done for each test material and control, and five seeds were planted per pot. The pots were conditioned in the greenhouse facility at Michigan State University (Plant Science Department) at 25 ± 3 °C during the day and 20 ± 3 °C during the night. A photoperiod of 16 h light followed by 8 h darkness was adopted at a luminance of 350 ± 50 μE m^{-2} s^{-1}, measured at the top of the canopy. The number of emergence, the biomass measurements (shoot dry weight and fresh weight) and the shoot height of the plants as a percentage of the controls are reported after 21 d of testing.

4. Results and discussion

Table 2 presents the average values, and their respective standard deviation, for $L^*a^*b^*$ indexes, gloss and hardness for (BA,AA)-PBAT/TPS films and (BA,AA)-*color* + {CoSt or CeSt} coated films.

PBAT is susceptible to photo-degradation due to the presence of benzene rings and carbonyl groups that are photosensitizers (Kijchavengkul et al., 2008, 2011). Benzene rings can absorb UV photons, but they are also capable of dissipating the absorbed UV energy by electronic delocalization. Carbonyl groups can absorb UV light and start the generation of free radicals by Norrish type I and type II reactions. Due to these multi-step mechanisms, the free-formed radicals will recombine and give rise to a cross-linked material. This process of recombination will then reduce ductility and the film will become more brittle and rigid (Kijchavengkul et al., 2011). Table 2 shows an increase in the average values for both gloss and hardness for the studied blend after UV aging due to the formation of a cross-linked structure. An increase in cross-linked structures has been demonstrated to inhibit the biodegradation process when a PBAT polymeric film comes into contact with microorganisms; the cross-linked domains make the film more rigid, limiting the access of water and microorganisms to the polymeric network (Kijchavengkul et al., 2011).

Table 2 shows that the UV-exposed PBAT/TPS films without coating had a small increase in lightness (L^* index) and the changes for the color-component coordinates (a^* and b^*), indicated reddish to greener and yellow to bluish tendencies, respectively. This difference among samples exposed to UV light and the unexposed samples can be explained by the presence of chromophoric groups on the PBAT/TPS structure that are able to absorb energy at the exposed UV wavelength causing an alteration in the $L^*a^*b^*$ indexes (Kijchavengkul et al., 2008, 2011).

For the coated samples, our discussion will center on three main points: i) effect of the substrate; ii) effect of the pigment; and iii) effect of the pro-degrading agent on both coating and substrate degradation.

Effect of the substrate: Exposure to UV light caused meaningful changes in the $L^*a^*b^*$ indexes for the PBAT/TPS blend because of the presence of chromophore groups on its structure, as mentioned above. For the uncoated and clear samples, the L^* values similarly increased for both aged materials, whereas a^* values decreased and b^* values increased. After an opaque pigment layer such as red, blue and black was applied to the surface, the differences among the measured $L^*a^*b^*$ parameters, gloss and hardness for the un-aged and aged films were less pronounced, indicating that the coating layer had a great effect on protecting the substrate from UV exposure.

Effect of the pigment: Sample behavior during UV exposure depended on the different chromophore group(s) present in each pigment. Table 2 shows that the clear coated samples had higher L^* (lightness) and b^* (yellowish) values and greater hardness after UV aging, but a lower gloss index. This result suggests that the sample was degraded by UV exposure, as indicated by increased yellowness on the film surface. As a consequence of degradation, the surface structure also became more brittle as evidenced by the increased hardness of the samples and the lower average gloss values.

In film samples coated with carbon black, light transmission was blocked by the ink layer, which caused two different effects that also have been described by other researchers (Kijchavengkul et al., 2008, 2011; Kroll et al., 2010; Wang and Hsieh, 2007): increases in the substrate temperature and inhibition of photo-degradation. These effects may happen during both UV curing and UV aging. UV curing and aging will work in a complementary way as a function of time, because during curing the exposure time is very short but the light intensity is extremely high when compared with UV exposure in the QUV chamber. So, the UV aging process induces a competition between curing and degradation, or more appropriately, between UV aging and UV complementary curing. The term "complementary curing" is used to describe the interaction of a reactive species immobilized in the cross-linked structure during the fast UV curing process. In the same way, the behavior of blue and black inks can be attributed to these main characteristics, which did not meaningfully impact the $L^*a^*b^*$ indexes, but increased the gloss index, and promoted a minor effect on hardness, impacting the 3D-structure and starting the photo-degradation on the ink layer.

For the red ink formulation, the photo-degradation generates Fe^{3+}, which are organic complexes in the azo region of the pigment. The predominance of a degradation mechanism involving charge transfer from ligand to metal when the molecule is irradiated by García-Montaño et al. (2008). The first degradation step is expected to attack the naphthalene ring, and therefore the overall degradation mechanism is slower than the one for simpler chemical structures. So, the parameters analyzed before and after aging in this study were not meaningfully changed in the red ink coated films by the UV light during the exposure time.

The yellow pigment formulations have been shown to be susceptible to UV light degradation due to the derivatives of oxalic acid diarylide, considered as a strong UV absorber (Bardi and Machado, 2012; Czajkowski and Paluszkiewicz, 2008). A considerable shifting

Table 2
Color, gloss and hardness values obtained for (BA,AA)-PBAT/TPS films and (BA,AA)-*color* + {CoSt or CeSt} coated films.

Film	L^*	a^*	b^*	Gloss	Hardness
BA-PBAT/TPS	80.1 ± 0.2^{a}	3.7 ± 0.1^{a}	16.4 ± 0.1^{a}	27.6 ± 5.0^{a}	47.7 ± 2.1^{a}
AA-PBAT/TPS	84.5 ± 0.4^{b}	1.3 ± 0.1^{b}	10.7 ± 0.4^{b}	47.0 ± 2.5^{b}	63.0 ± 1.7^{b}
BA-*Clear*	80.7 ± 0.2^{a}	−0.7 ± 0.1^{ab}	5.2 ± 0.1^{a}	77.2 ± 13.6^{a}	50.0 ± 3.0^{abc}
AA-*Clear*	89.3 ± 1.0^{b}	−0.8 ± 0.1^{b}	13.4 ± 2.9^{b}	45.6 ± 38.6^{ab}	59.3 ± 2.1^{ab}
BA-*Clear* + CoSt	80.4 ± 0.2^{a}	−0.5 ± 0.2^{a}	5.2 ± 0.3^{a}	9.6 ± 2.0^{b}	39.3 ± 0.6^{c}
AA-*Clear* + CoSt	88.2 ± 0.1^{b}	−0.7 ± 0.1^{ab}	16.4 ± 0.1^{b}	29.3 ± 9.0^{ab}	42.3 ± 10.8^{bc}
BA-*Clear* + CeSt	79.5 ± 0.2^{a}	−1.2 ± 0.1^{c}	7.3 ± 0.2^{a}	11.4 ± 0.5^{b}	66.7 ± 11.0^{a}
AA-*Clear* + CeSt	86.3 ± 1.1^{c}	−0.3 ± 0.1^{a}	23.7 ± 1.6^{c}	60.5 ± 34.0^{ab}	96.3 ± 7.1^{d}
BA-*Red*	39.9 ± 0.4^{ab}	41.3 ± 0.3^{ab}	21.9 ± 0.4^{a}	18.6 ± 1.6^{ab}	45.7 ± 2.5^{ab}
AA-*Red*	38.1 ± 0.6^{c}	38.4 ± 0.9^{c}	20.5 ± 0.8^{ab}	18.3 ± 2.3^{b}	47.7 ± 0.6^{ab}
BA-*Red* + CoSt	39.1 ± 0.6^{bc}	41.9 ± 0.6^{a}	21.0 ± 0.8^{ab}	27.1 ± 1.1^{a}	49.7 ± 2.5^{ac}
AA-*Red* + CoSt	38.6 ± 0.3^{c}	39.9 ± 0.3^{bc}	20.2 ± 0.1^{b}	15.6 ± 0.7^{b}	64.7 ± 2.1^{d}
BA-*Red* + CeSt	40.3 ± 0.1^{a}	41.9 ± 0.2^{a}	21.7 ± 0.3^{a}	15.4 ± 1.4^{b}	43.3 ± 0.6^{b}
AA-*Red* + CeSt	38.5 ± 0.3^{c}	39.0 ± 0.5^{c}	20.0 ± 0.5^{b}	14.6 ± 7.0^{b}	53.7 ± 2.3^{c}
BA-*Blue*	33.5 ± 0.3^{a}	−3.5 ± 0.3^{a}	−29.3 ± 0.3^{a}	24.7 ± 1.9^{a}	50.7 ± 0.6^{a}
AA-*Blue*	33.9 ± 0.5^{ab}	−3.7 ± 0.7^{a}	−31.2 ± 0.3^{b}	45.1 ± 1.5^{b}	67.0 ± 6.0^{b}
BA-*Blue* + CoSt	33.9 ± 0.3^{ab}	−5.0 ± 0.7^{ab}	−30.4 ± 0.3^{b}	34.6 ± 5.7^{c}	48.3 ± 1.5^{a}
AA-*Blue* + CoSt	34.8 ± 0.4^{b}	−4.2 ± 0.7^{ab}	−32.0 ± 0.3^{c}	25.8 ± 1.2^{a}	63.0 ± 0.0^{bc}
BA-*Blue* + CeSt	33.9 ± 0.3^{ab}	−5.7 ± 0.3^{b}	−30.9 ± 0.2^{b}	22.9 ± 1.4^{a}	51.0 ± 5.6^{a}
AA-*Blue* + CeSt	34.9 ± 0.3^{b}	−5.3 ± 0.4^{b}	−32.5 ± 0.2^{c}	40.3 ± 4.4^{bc}	55.7 ± 1.1^{ac}
BA-*Black*	25.4 ± 0.1^{a}	2.1 ± 0.1^{a}	−0.5 ± 0.1^{ab}	36.1 ± 15.5^{a}	51.7 ± 1.5^{a}
AA-*Black*	25.0 ± 0.4^{a}	1.9 ± 0.1^{b}	−0.5 ± 0.2^{ab}	41.2 ± 2.4^{a}	53.0 ± 2.0^{a}
BA-*Black* + CoSt	24.6 ± 0.4^{a}	1.8 ± 0.1^{b}	−1.3 ± 0.3^{c}	33.0 ± 10.6^{a}	45.0 ± 2.0^{a}
AA-*Black* + CoSt	25.2 ± 0.3^{a}	1.9 ± 0.1^{ab}	−0.6 ± 0.2^{ab}	20.1 ± 5.4^{a}	67.3 ± 4.5^{b}
BA-*Black* + CeSt	25.0 ± 0.1^{a}	2.0 ± 0.1^{ab}	−0.9 ± 0.1^{bc}	22.9 ± 1.0^{a}	49.3 ± 4.7^{a}
AA-*Black* + CeSt	24.8 ± 1.0^{a}	2.0 ± 0.1^{ab}	−0.2 ± 0.2^{a}	41.2 ± 5.0^{a}	52.3 ± 1.1^{a}
BA-*White*	86.9 ± 0.7^{abc}	1.9 ± 0.5^{a}	4.8 ± 0.5^{a}	39.7 ± 2.3^{a}	51.3 ± 0.6^{a}
AA-*White*	88.2 ± 0.2^{d}	0.8 ± 0.1^{b}	5.1 ± 0.1^{a}	51.4 ± 3.5^{b}	56.7 ± 2.3^{b}
BA-*White* + CoSt	86.5 ± 0.1^{b}	1.8 ± 0.1^{a}	4.9 ± 0.3^{a}	23.3 ± 4.3^{cd}	51.3 ± 0.6^{a}
AA-*White* + CoSt	87.7 ± 0.1^{cd}	1.0 ± 0.1^{b}	4.3 ± 0.2^{a}	26.0 ± 1.1^{ce}	62.7 ± 1.5^{c}
BA-*White* + CeSt	86.7 ± 0.5^{ab}	1.2 ± 0.1^{b}	5.9 ± 3.4^{a}	18.1 ± 1.0^{d}	50.0 ± 2.0^{a}
AA-*White* + CeSt	87.6 ± 0.1^{bcd}	0.9 ± 0.1^{b}	4.8 ± 0.1^{a}	31.5 ± 1.4^{e}	54.0 ± 2.6^{ab}
BA-*Yellow*	74.6 ± 0.3^{ab}	10.8 ± 0.2^{a}	72.9 ± 0.4^{a}	32.0 ± 2.9^{a}	50.7 ± 0.6^{a}
AA-*Yellow*	75.6 ± 0.1^{c}	12.1 ± 0.2^{b}	79.1 ± 0.8^{b}	37.9 ± 2.8^{a}	62.7 ± 1.5^{b}
BA-*Yellow* + CoSt	74.0 ± 0.2^{b}	7.5 ± 0.8^{c}	55.5 ± 1.3^{c}	36.0 ± 3.0^{a}	30.0 ± 0.0^{c}
AA-*Yellow* + CoSt	78.7 ± 0.5^{d}	13.6 ± 0.6^{d}	85.9 ± 1.0^{d}	35.6 ± 13.6^{a}	34.0 ± 2.6^{d}
BA-*Yellow* + CeSt	75.0 ± 0.1^{ac}	10.7 ± 0.4^{a}	74.1 ± 0.7^{a}	26.6 ± 3.2^{a}	48.0 ± 1.0^{b}
AA-*Yellow* + CeSt	76.4 ± 0.2^{e}	11.1 ± 0.3^{ab}	82.3 ± 0.2^{e}	37.3 ± 0.7^{a}	60.3 ± 1.1^{a}

Note: Values are given as means ± SD. Values in the same column for the same color (i.e., clear, red), with same lower superscript letters are not significantly different at type I error (α) of 0.05, using the Tukey–Kramer test.

to yellow on the b^* coordinate and an increase in the hardness value was observed in this study. The so-called residual curing process may have also taken part during the exposure to UV aging, and this resulted in an increased value for gloss index.

Effect of the pro-degrading agent: The incorporation of CoSt and CeSt caused similar changes in the color of the developed inks after aging. AA-*Clear* + (CoSt, CeSt), AA-*Yellow* + (CoSt, CeSt) and AA-*Red* + (CoSt, CeSt) films became slightly lighter, less reddish and more yellowish, when compared with the BA-*color* + (CoSt, CeSt) films. In contrast, AA-*Black* + (CoSt, CeSt), AA-*Blue* + (CoSt, CeSt) and AA-*White* + (CoSt, CeSt) had no change in the L^* and a^* parameters during the aging period. According to various researchers (Campardelli et al., 2014; Hoppe et al., 2010; Shenoy and Bowman, 2010), carbon black and titanium dioxide tend to protect the sample from absorbing UV photons in specific test conditions. In this study, the average values for gloss increased for the clear coating and white ink samples, but decreased for the red and blue ink samples. This result may suggest that two components – photo-initiator and pro-degrading agents – are competing for the photons during the curing process. Some properties of the final cured materials could have been affected, especially gloss, which is a very good indicator of the degree of curing (Bardi and Machado, 2012).

Table 3 presents the average values for the thermal properties and average molecular weight of PBAT for (BA,AA)-PBAT/TPS films and (BA,AA)-*color* + {CoSt or CeSt}.

PBAT/TPS blends show two glass transitions. A T_g around -35 °C corresponds to the PBAT region, whereas the transition just above room temperature is correlated to the TPS rich phase (Olivato et al., 2013; Signori et al., 2009). Some authors reported that the T_m for PBAT normally ranges from 110 °C to 115 °C, but, in this study, we observed temperatures in the order of 145 °C, suggesting a very strong interaction between the TPS and PBAT phases by means of the compatibilizing agents (Pye and Roth, 2011; Weng et al., 2013). Furthermore, Table 3 shows that the T_g, T_m and melting enthalpy (H_m), for BA-*color* samples, did not vary in a meaningful way, implying that the coating layer and pro-degrading additives did not interfere with the thermal behavior of the substrate in the tested conditions. When analyzing the data for the samples exposed to UV-aging in the QUV chamber during 250 h, it was possible to verify that the pigmented compositions, especially the red, blue and yellow containing CoSt, had a slight reduction in the T_g associated with the PBAT rich phase.

To investigate the influence of the coating and the additive on the abiotic degradation of the samples, GPC was performed and the results are reported in Table 3. The average values of $\bar{M}_w$ and $\bar{M}_n$ for BA-PBAT/TPS are similar to previous work (Chen and Zhang, 2009; Dong et al., 2013; Kijchavengkul et al., 2010a,b; Ma et al., 2012; Oyama et al., 2011; Signori et al., 2009). A reduction in $\bar{M}_w$ and $\bar{M}_n$ values was found when samples were exposed to UV radiation. The irradiation can start the reduction of the molecular weight

Table 3
Values for the thermal properties and for average molecular weight of PBAT for (BA,AA)-PBAT/TPS films and (BA,AA)-*color* + {CoSt or CeSt} coated films.

Material	T_g 1 (°C)	T_g 2 (°C)	T_c (°C)	H_c (J g^{-1})	T_m (°C)	H_m (J g^{-1})	M_w (10^3 Da)	M_n (10^3 Da)
BA-PBAT/TPS	−28.5 ± 6.4^{a}	39.1 ± 12.8^{a}	80.7 ± 8.6^{a}	10.7 ± 0.6^{a}	149.9 ± 0.7^{a}	4.9 ± 0.6^{a}	71.1 ± 2.7^{a}	40.4 ± 9.1^{a}
AA-PBAT/TPS	−29.8 ± 3.4^{a}	44.6 ± 11.4^{a}	79.6 ± 1.7^{a}	8.9 ± 1.2^{a}	145.4 ± 1.4^{b}	6.3 ± 0.7^{a}	34.7 ± 19.8^{a}	14.5 ± 5.5^{a}
BA-*Clear*	−23.3 ± 0.5^{a}	40.2 ± 17.0^{a}	77.7 ± 2.4^{a}	7.8 ± 1.4^{a}	141.5 ± 15.4^{a}	3.5 ± 0.3^{a}	50.2 ± 24.4^{a}	24.5 ± 7.6^{a}
AA-*Clear*	−20.0 ± 2.1^{b}	48.9 ± 0.4^{a}	*	*	148.6 ± 0.3^{a}	2.7 ± 0.5^{a}	66.4 ± 4.3^{a}	10.2 ± 7.5^{b}
BA-*Clear* + CoSt	−22.3 ± 2.8^{ab}	*	79.4 ± 1.7^{a}	3.1 ± 0.6^{b}	*	*	61.4 ± 4.0^{a}	28.2 ± 1.7^{a}
AA-*Clear* + CoSt	−25.3 ± 3.4^{b}	*	*	*	*	*	7.3 ± 0.0^{b}	4.6 ± 1.1^{b}
BA-*Clear* + CeSt	−26.7 ± 2.4^{b}	*	*	*	*	*	42.3 ± 19.9^{ab}	33.4 ± 3.7^{a}
AA-*Clear* + CeSt	−25.1 ± 3.4^{b}	*	*	*	*	*	42.6 ± 2.3^{ab}	18.5 ± 4.3^{abc}
BA-*Red*	−23.9 ± 3.0^{a}	46.2 ± 14.9^{a}	82.3 ± 4.2^{a}	9.6 ± 0.9^{a}	146.0 ± 8.0^{a}	5.8 ± 0.4^{a}	22.9 ± 1.5^{a}	14.8 ± 2.0^{a}
AA-*Red*	−25.5 ± 3.1^{a}	52.8 ± 5.9^{ab}	81.7 ± 1.7^{a}	10.3 ± 1.2^{a}	147.2 ± 0.8^{a}	7.6 ± 0.6^{b}	30.9 ± 0.8^{b}	18.6 ± 0.6^{a}
BA-*Red* + CoSt	−19.6 ± 3.0^{ab}	54.9 ± 0.8^{ab}	84.7 ± 0.5^{a}	9.8 ± 0.4^{a}	146.0 ± 1.4^{a}	4.7 ± 1.8^{a}	21.8 ± 2.5^{a}	14.9 ± 3.7^{a}
AA-*Red* + CoSt	−17.9 ± 3.1^{b}	54.3 ± 5.9^{ab}	85.3 ± 1.7^{a}	10.0 ± 1.2^{a}	146.0 ± 0.8^{a}	4.6 ± 0.6^{a}	22.3 ± 1.3^{a}	13.4 ± 2.9^{a}
BA-*Red* + CeSt	−17.1 ± 3.0^{b}	51.3 ± 14.9^{ab}	83.5 ± 4.2^{a}	10.2 ± 0.9^{a}	138.6 ± 8.0^{a}	10.2 ± 0.4^{c}	24.0 ± 0.6^{a}	14.8 ± 0.3^{a}
AA-*Red* + CeSt	−23.1 ± 0.5^{a}	48.7 ± 8.6^{ab}	82.6 ± 1.7^{a}	10.1 ± 1.2^{a}	143.7 ± 1.4^{a}	7.5 ± 0.7^{b}	22.3 ± 0.0^{a}	14.3 ± 0.0^{a}
BA-*Blue*	−23.3 ± 6.4^{a}	53.4 ± 12.8^{a}	81.1 ± 8.6^{a}	10.0 ± 0.6^{a}	145.4 ± 0.7^{ab}	6.2 ± 0.6^{a}	22.7 ± 0.1^{a}	11.5 ± 2.2^{a}
AA-*Blue*	−23.0 ± 0.9^{ab}	52.8 ± 1.6^{ab}	81.5 ± 0.1^{ab}	9.2 ± 1.0^{ab}	146.4 ± 1.2^{a}	6.7 ± 1.2^{ab}	22.4 ± 1.7^{a}	15.1 ± 3.9^{a}
BA-*Blue* + CoSt	−24.2 ± 6.4^{a}	51.1 ± 12.8^{a}	83.8 ± 8.6^{a}	9.8 ± 0.6^{a}	146.4 ± 0.7^{a}	6.4 ± 0.6^{ab}	23.1 ± 0.4^{a}	12.7 ± 2.0^{a}
AA-*Blue* + CoSt	−20.5 ± 2.0^{ab}	57.3 ± 5.6^{bc}	85.2 ± 1.4^{a}	8.9 ± 1.2^{b}	145.9 ± 1.0^{a}	6.1 ± 0.7^{a}	26.5 ± 4.7^{a}	13.4 ± 1.6^{a}
BA-*Blue* + CeSt	−23.2 ± 6.4^{a}	50.6 ± 12.8^{a}	82.1 ± 8.6^{a}	10.8 ± 0.6^{c}	144.6 ± 0.7^{ab}	6.8 ± 0.6^{b}	23.6 ± 0.8^{a}	14.0 ± 1.9^{a}
AA-*Blue* + CeSt	−22.9 ± 4.4^{a}	53.0 ± 9.1^{a}	82.7 ± 5.5^{a}	9.7 ± 0.8^{b}	145.7 ± 0.9^{a}	6.4 ± 0.7^{ab}	24.4 ± 3.2^{a}	14.2 ± 2.9^{a}
BA-*Black*	−27.0 ± 2.8^{a}	50.7 ± 5.3^{a}	84.3 ± 0.9^{a}	9.8 ± 0.4^{a}	146.1 ± 2.1^{ab}	5.6 ± 1.6^{a}	23.5 ± 1.1^{a}	14.1 ± 2.0^{a}
AA-*Black*	−18.3 ± 2.8^{b}	59.6 ± 5.6^{ab}	86.6 ± 1.9^{ab}	10.6 ± 1.2^{ab}	144.1 ± 0.8^{a}	7.2 ± 0.7^{ab}	17.9 ± 1.8^{b}	11.4 ± 2.0^{a}
BA-*Black* + CoSt	−25.2 ± 6.4^{ab}	57.1 ± 11.4^{ab}	84.7 ± 8.6^{abc}	8.8 ± 0.6^{c}	144.3 ± 0.7^{a}	1.8 ± 0.6^{c}	22.7 ± 0.4^{a}	13.1 ± 1.2^{a}
AA-*Black* + CoSt	−24.2 ± 5.2^{ab}	56.2 ± 9.^{8ab}	86.9 ± 1.7^{ab}	10.3 ± 1.2^{ab}	143.8 ± 1.4^{a}	2.2 ± 0.7^{c}	17.3 ± 1.8^{b}	11.8 ± 3.1^{a}
BA-*Black* + CeSt	−33.0 ± 6.4^{bc}	56.3 ± 12.8^{ab}	86.0 ± 8.6^{ab}	9.8 ± 0.6^{a}	148.0 ± 0.7^{b}	3.3 ± 0.6^{c}	22.1 ± 0.2^{a}	10.4 ± 1.2^{a}
AA-*Black* + CeSt	−27.2 ± 5.0^{bc}	52.3 ± 2.0^{ab}	83.5 ± 1.0^{ab}	9.6 ± 0.3^{a}	146.2 ± 1.0^{a}	6.3 ± 0.4^{ab}	18.6 ± 1.0^{b}	11.6 ± 2.5^{a}
BA-*White*	−23.0 ± 3.9^{a}	48.2 ± 6.2^{a}	80.6 ± 0.8^{a}	9.4 ± 0.5^{a}	144.4 ± 0.3^{a}	5.8 ± 1.1^{a}	24.7 ± 1.0^{a}	13.2 ± 2.3^{a}
AA-*White*	−19.9 ± 2.0^{ab}	49.7 ± 1.6	82.9 ± 0.8^{b}	10.0 ± 0.6^{ab}	146.1 ± 1.0^{b}	6.4 ± 1.0^{ab}	18.6 ± 0.0^{bc}	9.1 ± 0.1^{b}
BA-*White* + CoSt	−26.9 ± 4.4^{ac}	51.2 ± 12.2^{a}	82.6 ± 5.2^{ab}	9.8 ± 0.7^{ab}	146.5 ± 3.7^{ab}	6.6 ± 0.7^{ab}	25.3 ± 0.1^{a}	17.1 ± 0.0^{a}
AA-*White* + CoSt	−21.7 ± 2.8^{ab}	51.0 ± 4.2^{a}	83.2 ± 0.7^{bc}	10.0 ± 0.4^{ab}	145.1 ± 0.3^{b}	6.6 ± 0.0^{b}	19.9 ± 0.0^{b}	11.0 ± 0.1^{a}
BA-*White* + CeSt	−19.5 ± 2.4^{ab}	53.6 ± 4.0^{ab}	84.4 ± 1.9^{cd}	9.5 ± 0.8^{a}	145.4 ± 1.4^{ab}	5.6 ± 1.5^{a}	23.7 ± 0.5^{a}	12.6 ± 1.1^{a}
AA-*White* + CeSt	−22.4 ± 3.7^{a}	56.8 ± 5.7^{ab}	85.4 ± 1.2^{cd}	9.2 ± 1.0 ^{a}	145.4 ± 1.1^{ab}	6.7 ± 0.7^{ab}	17.4 ± 0.0^{c}	7.3 ± 0.1^{b}
BA-*Yellow*	−18.2 ± 2.8^{a}	54.5 ± 5.4^{a}	84.4 ± 3.0^{a}	9.9 ± 0.6^{a}	145.6 ± 1.9^{a}	6.5 ± 1.1^{a}	22.1 ± 1.3^{a}	14.8 ± 0.2^{a}
AA-*Yellow*	−22.4 ± 1.9^{ab}	50.3 ± 3.8^{ab}	81.3 ± 1.2^{b}	9.5 ± 0.1^{a}	145.9 ± 0.1^{a}	6.2 ± 0.2^{a}	24.3 ± 1.4^{a}	17.9 ± 1.2^{ab}
BA-*Yellow* + CoSt	−23.2 ± 1.2^{b}	57.3 ± 0.3^{c}	81.0 ± 0.9^{b}	6.7 ± 0.6^{b}	149.9 ± 0.5^{b}	2.4 ± 1.5^{b}	33.9 ± 0.3^{b}	22.7 ± 0.9^{b}
AA-*Yellow* + CoSt	−17.3 ± 3.3^{ab}	56.1 ± 5.7^{abc}	92.7 ± 1.7^{c}	6.3 ± 0.9^{b}	149.6 ± 1.0^{b}	3.3 ± 0.7^{b}	27.3 ± 2.1^{b}	20.1 ± 1.8^{a}
BA-*Yellow* + CeSt	−26.3 ± 4.5^{bc}	57.1 ± 10.6^{abc}	84.5 ± 5.2^{ab}	11.6 ± 0.7^{c}	144.5 ± 3.4^{a}	2.2 ± 0.8^{b}	25.4 ± 0.8^{a}	18.7 ± 0.5^{b}
AA-*Yellow* + CeSt	−19.4 ± 3.0^{ab}	55.9 ± 4,8^{a}	86.9 ± 1.2^{a}	9.2 ± 0.9^{a}	147.9 ± 1.^{0ab}	2.2 ± 0.6^{b}	22.8 ± 0.8^{a}	15.2 ± 1.5^{a}

Note: Values are given as means ± SD. Values in the same column for the same color (i.e., clear, red), with same lower superscript letters are not statistically significantly different at type I error (α) of 0.05, using the Tukey–Kramer test.

of polyesters by attacking the interface between crystalline and amorphous phase (Chen et al., 2011). In the case of PBAT, the crystalline phase is randomly dispersed on the polymeric matrix, which makes the photo-degradation process more complex to predict (Chen et al., 2011). A large reduction in $\bar{M}_w$ and $\bar{M}_n$ was observed for the samples coated with red, blue, black, white and yellow inks. This result may be attributed to a synergistic effect mainly catalyzed by the pigments. Reduction after UV exposure was not very large, and in many cases not statistically significant. Similar behaviors were observed for the pigmented samples and for the ones containing the pro-degrading additives, indicating that these components have little influence on the randomly-assumed degradation process for PBAT and TPS compared with polyolefins (Hopewell et al., 2009; Thompson et al., 2009; Ojeda, 2013).

A subset of the samples, BA-PBAT/TPS, AA-PBAT/TPS, AA-*Black*, AA-*Black* + CoSt, AA-*Yellow*, AA-*Yellow* + CoSt, were exposed to a laboratory-controlled biodegradation test under manure compost. Only samples containing CoSt were evaluated because of their improved mechanical, optical and thermal properties after UV-aging when compared with the samples containing CeSt. Table 4 shows the values for sample mineralization after 21, 42 and 63 d as calculated in Eq. (1). Fig. 2 shows the average values (in g) for CO_2 evolution for the tested samples during 63 d of exposure in manure compost under controlled conditions.

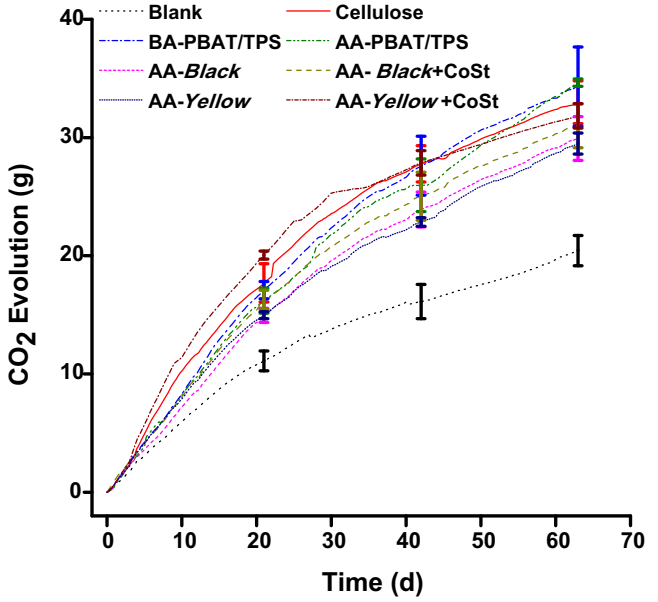

Fig. 2. Average values, and their respective standard deviations, for CO_2 evolution during biodegradation for the selected samples.

Table 4
Values for the mineralization, thermal properties and for average molecular weight of PBAT for (BA,AA)-PBAT/TPS films and (BA,AA)-*color* + {CoSt} coated films after biodegradation test.

Material	Mineralization in % after...		M_w (10^3 Da)	M_n (10^3 Da)	T_g 1 (°C)	T_g 2 (°C)	T_c (°C)	H_c (J g^{-1})	T_m (°C)	H_m (J g^{-1})
	21 d	42 d	63 d							
Cellulose (control)	49.6 ± 13.8^{ab}	87.7 ± 15.8^{a}	94.5 ± 16.6^{ab}	NA	NA	NA	NA	NA	NA	NA
BA-PBAT/TPS	36.9 ± 6.9^{bc}	71.1 ± 17.8^{ab}	85.8 ± 22.2^{ab}	5.4 ± 0.3^{a}	1.9 ± 0.5^{a}	−23.1 ± 6.3^{a}	72.9 ± 19.5^{a}	108.9 ± 3.5^{a}	3.2 ± 1.1^{a}	138.1 ± 3.3^{a}	2.7 ± 1.0^{a}
AA-PBAT/TPS	37.2 ± 14.6^{bc}	70.0 ± 28.0^{ab}	104.0 ± 31.5^{a}	4.4 ± 0.1^{b}	0.3 ± 0.1^{b}	−18.8 ± 4.7^{a}	78.0 ± 11.1^{a}	113.1 ± 4.6^{a}	2.0 ± 0.5^{a}	140.9 ± 5.6^{a}	2.1 ± 0.5^{a}
AA-Black	24.3 ± 6.9^{c}	49.3 ± 13.8^{ab}	60.0 ± 15.1^{ab}	2.6 ± 0.5^{c}	0.2 ± 0.1^{b}	−20.2 ± 3.6^{a}	80.9 ± 5.5^{a}	102.1 ± 2.5^{a}	3.3 ± 1.8^{a}	137.9 ± 1.0^{a}	3.7 ± 1.6^{a}
AA-Black + CoSt	31.4 ± 7.3^{bc}	54.2 ± 15.3^{ab}	64.2 ± 13.9^{ab}	3.6 ± 0.2^{d}	2.0 ± 0.5^{a}	−18.8 ± 0.5^{a}	73.1 ± 0.2^{a}	108.8 ± 3.5^{a}	1.9 ± 1.1^{a}	126.7 ± 3.3^{a}	2.3 ± 1.0^{a}
AA-Yellow	28.1 ± 11.7^{c}	49.3 ± 20.2^{b}	66.2 ± 25.6^{ab}	2.0 ± 0.3^{c}	0.4 ± 0.1^{b}	−21.7 ± 1.9^{a}	58.2 ± 9.7^{a}	115.1 ± 3.5^{a}	3.5 ± 1.1^{a}	138.1 ± 3.3^{a}	5.4 ± 1.0^{a}
AA-Yellow + CoSt	54.7 ± 7.7^{a}	64.5 ± 12.7^{a}	67.7 ± 13.4^{b}	0.0 ± 0.0^{e}	0.0 ± 0.0^{b}	−17.0 ± 3.4^{a}	86.4 ± 9.2^{a}	110.9 ± 3.5^{a}	4.5 ± 1.1^{a}	144.7 ± 3.3^{a}	4.5 ± 1.0^{a}

Note: Values are given as means ± SD. Values in the same column with same lower superscript letters are not statistically significantly different at type I error (α) of 0.05, using the Tukey–Kramer test. NA = Not applicable.

Table 5
Average values for the germinated seeds of *Lepidium sativum* in supernatant collected from the compost after biodegradation for the selected polymeric films, cellulose, blank and control (pure water) after 4 days in the dark at 23 ± 3 °C.

Substance	Lepidium sativum	
	Total germinated seeds (%)	Germinated seeds (%) relative to the control
Water (control)	95.0 ± 10.0	–
Blank	90.0 ± 20.0	94.7
Cellulose	85.0 ± 19.1	89.5
AA-PBAT/TPS	95.0 ± 10.0	100.0
AA-Yellow	90.0 ± 20.0	94.7

Fig. 2 shows that the PBAT/TPS films produced similar amounts of carbon dioxide as did cellulose, the positive control. Degradation occurs mainly due to microbial degradation and hydrolysis preferentially on the non-crystalline domain, the predominant regions in both PBAT and TPS (Kijchavengkul et al., 2010a; Muniyasamy et al., 2013; Weng et al., 2013). The film samples are composed of two biodegradable materials with TPS as the dispersed phase and PBAT as the continuous phase (Stagner et al., 2012). The bioassimilation process occurs by two competitive and enzyme-specific mechanisms for PBAT and TPS (Ren et al., 2009). A slight difference between the mineralization values (Table 4) was observed for BA-PBAT/TPS and AA-PBAT/TPS at 63 d. However, the high variability of the biological tests made it difficult to reach an overall conclusion from the CO_2 evolution. Both samples had a meaningful reduction in both $\bar{M}_w$ and $\bar{M}_n$ compared with their initial values from Table 3. However, the AA-PBAT/TPS sample showed a final lower $\bar{M}_w$ and $\bar{M}_n$ at 63 d, indicating that the microorganisms can easily digest the lower $\bar{M}_w$ and $\bar{M}_n$ of the PBAT samples.

The biodegradation of the coated films (Table 4), independently of the pigment, resulted in lower final mineralization values. However, the $\bar{M}_w$ and $\bar{M}_n$ remained almost the same due to the low initial values. The relatively high cross-linked structure of the polymeric coatings may offer resistance to the microorganisms to reach the polymeric bulk of the substrate, once the available surface area for microbiological adhesion is reduced. According to Neoh and Kang (2011), epoxy-resin derived materials are very efficient at protecting their substrate from biocorrosion and biodegradation.

The additives did not influence on the biodegradation of the colored materials. The AA-*Black* sample shows some $\bar{M}_w$ and $\bar{M}_n$ differences when compared to the AA-*Black* + CoSt, which can be associated to the capacity of carbon black to absorb UV photons. The $\bar{M}_w$ and $\bar{M}_n$ values for AA-*Yellow* + CoSt were significantly lower than those for AA-*Yellow* (Table 4), suggesting that the CoSt may play a role in allowing the microorganisms to reach the polymeric bulk and breaking it down. Table 4 shows that thermal properties for the studied samples had large variability and were not statistically different before and after the biodegradation process.

To evaluate the quality of the compost after the biodegradation of the selected samples, seeds were allowed to germinate in a liquid medium (or supernatant) and in a mixture of compost and potting soil. Table 5 summarizes the data obtained from the germination test and Table 6 provides plant growth test data.

No meaningful differences in seed germination were found during the germination time in the supernatant for any of the analyzed samples when compared with the control (Table 5). The same can be said about the plants grown during 21 days at the greenhouse, except for the result with AA-*Yellow* + CoSt (Table 6). The small amount of CoSt in that sample seemed to cause a positive effect on both plant species in the plant growth test. Cobalt derivatives are regarded as a beneficial element for plants, which varies for each species. The low availability of cobalt in soils leads to disorders in ruminant livestock (Uren, 2013) although excessive exposure can

Table 6
Average values from the plant growth test with *Cucumis sativus* and *Avena sativa* using the compost after biodegradation for the selected polymeric films, cellulose and blank (control) 21 days after germination.

Substance	*Cucumis sativus*					*Avena sativa*				
	Total germinated seeds (%)	Germinated seeds relatively to the control (%)	Height (cm)	Wet weight (g)	Dry weight (g)	Total germinated seeds (%)	Germinated seeds relatively to the control (%)	Height (cm)	Wet weight (g)	Dry weight (g)
Blank (control)	$68.0 \pm 10.9^{A^*}$	–	$3.9 \pm 0.5^{A^*}$	$2.06 \pm 1.14^{A^*}$	$0.35 \pm 0.22^{A^*}$	$72.0 \pm 10.9^{A^*}$	–	$4.8 \pm 5.0^{A^*}$	$0.28 \pm 0.53^{A^*}$	$0.05 \pm 0.09^{A^*}$
Cellulose	$80.0 \pm 0.0^{AB^*}$	118.0	$4.2 \pm 0.4^{A^*}$	$3.90 \pm 0.28^{A^*}$	$0.68 \pm 0.01^{A^*}$	$64.0 \pm 26.1^{A^*}$	89.0	15.9 ± 4.6^{BC}	$1.19 \pm 0.76^{AB^*}$	$0.21 \pm 0.13^{A^*}$
AA-PBAT/TPS	$68.0 \pm 17.9^{A^*}$	100.0	9.2 ± 4.0^{B}	$3.13 \pm 0.79^{A^*}$	$0.56 \pm 0.13^{A^*}$	$68.0 \pm 26.8^{A^*}$	94.0	$9.2 \pm 4.0^{AC^*}$	$0.25 \pm 0.15^{A^*}$	$0.04 \pm 0.02^{A^*}$
AA-Yellow	$68.0 \pm 10.9^{A^*}$	100.0	$4.2 \pm 0.3^{A^*}$	$3.46 \pm 1.34^{A^*}$	$0.61 \pm 0.27^{A^*}$	$80.0 \pm 0.0^{A^*}$	111.0	14.2 ± 6.5^{BC}	$0.73 \pm 0.52^{AB^*}$	$0.12 \pm 0.09^{A^*}$
AA-Yellow + CoSt	$68.0 \pm 10.0^{A^*}$	100.0	$6.9 \pm 1.1^{AB^*}$	12.22 ± 3.42^{B}	2.12 ± 0.58^{B}	$55.0 \pm 25.2^{A^*}$	79.0	22.8 ± 2.8^{B}	1.88 ± 0.99^{B}	0.57 ± 0.29^{B}

Note: Values for the total germinated seed are given as means ± SD. Values in the same column with same capital superscript letters are not statistically significantly different at type I error (α) of 0.05, using the Tukey–Kramer test. Values in the same column with star (*) superscript are not statistically significantly different from the control (water) using Dunnett's comparisons test.

cause an increase in the water content in the leaves in some species (Nagajyoti et al., 2010).

5. Conclusions

The properties of PBAT/TPS were dependent on the degree of curing of the clear coating, and the red, blue, black, white and yellow inks, without and with pro-degrading additives (i.e., CoSt and CeSt), printed on the film. These characteristics are directly related to the class of pigment incorporated into the formulation and its capacity to absorb UV photons. On the other hand, the presence of pro-degrading additives in the coating layer, at the concentration studied, does not play a beneficial role on accelerating the abiotic degradation during UV aging in the conditions evaluated in this study. Moreover, residual curing competed for UV photons during the exposure in the QUV chamber, which tended to reduce the overall biotic and abiotic degradation of the polymeric biodegradable substrate.

The PBAT/TPS films exposed to UV aging showed higher biodegradation than the cellulose used as a positive control. The presence of yellow ink together with CoSt had an effect on reducing the $\bar{M}_w$ of the polymeric blends. The presence of CoSt did not affect CO_2 production at 21, 42 and 63 days during the respirometric test. Additionally, the amount of CoSt did not have a detrimental effect on ecotoxicity during plant growth.

Acknowledgments

The authors thank the Fundação de Amparo à Pesquisa do Estado de São Paulo (FAPESP) for financial support (grant no. 2010/02631-0), and the Conselho Nacional de Desenvolvimento Científico e Tecnológico (CNPq) for scholarships. The authors acknowledge Flint Ink do Brasil S.A. (Cotia, SP, Brazil) for help in preparing the clear coating and print inks. The authors are grateful for the collaboration of Susan Selke, Ning Gong, Edgar Castro Aguirre, Rodolfo Lopez-Gonzalez, Rijosh John Cheruvathur and Tanatorn Tongsumrith during the direct measurement respirometry, germination test and plant growth, and Dave Freville for allowing the use of the greenhouse facility at MSU.

References

Al-Salem, S.M., Lettieri, P., Baeyens, J., 2009. Recycling and recovery routes of plastic solid waste (PSW). A review. Waste Manage. 29, 2625–2643.

Bardi, M.A.G., Machado, L.D.B., 2012. Accompanying of parameters of color, gloss and hardness on polymeric films coated with pigmented inks cured by different radiation doses of ultraviolet light. Rad. Phys. Chem. 81, 1332–1335.

Briassoulis, D., Dejean, C., Picuno, P., 2010. Critical review of norms and standards for biodegradable agricultural plastics Part II: Composting. J. Polym. Environ. 18, 364–383.

Campardelli, R., Porta, G.D., Gomez, V., Irusta, S., Reverchon, E., Santamaria, J., 2014. Au–PLA nanocomposites for photothermally controlled drug delivery. J. Mater. Chem. B 2, 409–417.

Chen, F., Zhang, J., 2009. A new approach for morphology control of poly(butylene adipate-co-terephthalate) and soy protein blends. Polymer 50, 3770–3777.

Chen, J.-H., Chen, C.-C., Yang, M.-C., 2011. Characterization of nanocomposites of poly(butylene adipate-co-terephthalate) blending with organoclay. J. Polym. Res. 18, 2151–2159.

Czajkowski, W., Paluszkiewicz, J., 2008. Synthesis of bifunctional monochlorotriazine reactive dyes increasing UV-protection properties of cotton fabrics. Fibres Textil East. Eur. 16, 122–126.

Dong, W., Zou, B., Yan, Y., Ma, P., Chen, M., 2013. Effect of chain-extenders on the properties and hydrolytic degradation behavior of the poly(lactide)/poly(butylene adipate-co-terephthalate) blends. Int. J. Mol. Sci. 14, 20189–20203.

García-Montaño, J., Torrades, F., Pérez-Estrada, L.A., Oller, I., Malato, S., Maldonado, M.I., Peral, J., 2008. Degradation pathways of the commercial reactive azo dye procion red H-E7B under solar-assisted photo-fenton reaction. Environ. Sci. Technol. 42, 6663–6670.

Hopewell, J., Dvorak, R., Kosior, E., 2009. Plastics recycling: challenges and opportunities. Phil. Trans. R. Soc. B 364, 2115–2126.

Hoppe, C.C., Ficek, B.A., Eom, H.S., Scranton, A.B., 2010. Cationic photopolymerization of epoxides containing carbon black nanoparticles. Polymer 51, 6151–6160.

Kijchavengkul, T., Auras, R., 2008. Compostability of polymers. Polym. Internat. 57, 793–804.
Kijchavengkul, T., Auras, R., Rubino, M., Ngouajio, M., Fernandez, R.T., 2006. Development of an automatic laboratory-scale respirometric system to measure polymer biodegradability. Polym. Test 25, 1006–1016.
Kijchavengkul, T., Auras, R., Rubino, M., 2008. Measuring gel content of aromatic polyesters using FTIR spectrophotometry and DSC. Polym. Test. 27, 55–60.
Kijchavengkul, T., Auras, R., Rubino, M., Alvarado, E., Montero, J.R.C., Rosales, J.M., 2010a. Atmospheric and soil degradation of aliphatic–aromatic polyester films. Polym. Degrad. Stab. 95, 99–107.
Kijchavengkul, T., Auras, R., Rubino, M., Selke, S., Ngouajio, M., Fernandez, R.T., 2010b. Biodegradation and hydrolysis rate of aliphatic aromatic polyester. Polym. Degrad. Stab. 95, 2641–2647.
Kijchavengkul, T., Auras, R., Rubino, M., Selke, S., Ngouajio, M., Fernandez, R.T., 2011. Formulation selection of aliphatic aromatic biodegradable polyester film exposed to UV/solar radiation. Polym. Degrad. Stab. 96, 1919–1926.
Kroll, M., Langer, B., Schumacher, S., Grellmann, W., 2010. The influence of carbon black batches on the fracture behavior of glass fiber reinforced PA6/PA66 blends. J. Appl. Polym. Sci. 116, 610–618.
Ma, P., Hristova-Bogaerds, D.G., Schimit, P., Goossens, J.G.P., Lemstra, P.J., 2012. Tailoring the morphology and properties of poly(lactic acid)/poly(ethylene)-co-(vinyl acetate)/starch blends via reactive compatibilization. Polym. Int. 61, 1284–1293.
Muniyasamy, S., Reddy, M.M., Misra, M., Mohanty, A., 2013. Biodegradable green composites from bioethanol co-product and poly(butylene adipate-co-terephthalate). Ind. Crops Prod. 43, 812–819.
Nagajyoti, P.C., Lee, K.D., Sreekanth, T.V.M., 2010. Heavy metals, occurrence and toxicity for plants: a review. Environ. Chem. Lett. 8, 199–216.
Neoh, K.G., Kang, E.T., 2011. Combating bacterial colonization on metals via polymer coatings: relevance to marine and medical applications. ACS Appl. Mater. Interfaces 3, 2808–2819.
Ojeda, T., 2013. Polymers and the environment. In: Yılmaz, F. (Ed.), Polymer Science. InTech Europe, Rijeka, pp. 1–34.
Olivato, J.B., Nobrega, M.M., Müller, C.M.O., Shirai, M.A., Yamasita, F., Grossmann, M.V.E., 2013. Mixture design applied for the study of the tartaric acid effect on starch/polyester films. Carbohydr. Polym. 92, 1705–1710.
Oyama, H.T., Tanaka, Y., Hirai, S., Shida, S., Kadosaka, A., 2011. Water-disintegrative and biodegradable blends containing poly(L-lactic acid) and poly(butylene adipate-co-terephthalate). J. Polym. Sci. Part B 49, 342–354.
Pye, J.E., Roth, C.B., 2011. Two simultaneous mechanisms causing glass transition temperature reductions in high molecular weight freestanding polymer films as measured by transmission ellipsometry. Phys. Rev. Lett. 107, 235701-1–235701-5.
Ren, J., Fu, H., Ren, T., Yuan, W., 2009. Preparation, characterization and properties of binary and ternary blends with thermoplastic starch, poly(lactic acid) and poly(butylene adipate-co-terephthalate). Carbohyd. Polym. 77, 576–582.
Roy, P.K., Hakkarainen, M., Varma, I.K., Albertsson, A.-C., 2010. Degradable polyethylene: fantasy or reality. Environ. Sci. Technol. 45, 4217–4227.
Shenoy, R., Bowman, C.N., 2010. Mechanism and implementation of oxygen inhibition suppression in photopolymerizations by competitive photoactivation of a singlet oxygen sensitizer. Macromolecules 43, 7964–7970.
Signori, F., Coltelli, M.-C., Bronco, S., 2009. Thermal degradation of poly(lactic acid) (PLA) and poly(butylene adipate-co-terephthalate) (PBAT) and their blends upon melt processing. Polym. Degrad. Stab. 94, 74–82.
Stagner, J.A., Alves, V.D., Narayan, R., 2012. Application and performance of maleated thermoplastic starch–poly(butylene adipate-co-terephthalate) blends for films. J. Appl. Polym. Sci. 126, E135–E142.
Thompson, R.C., Moore, C.J., vom Saal, F.S., Swan, S.H., 2009. Plastics, the environment and human health: current consensus and future trends. Phil. Trans. R. Soc. B 364, 2153–2156.
Uren, N.C., 2013. Cobalt and manganese. In: Alloway, B.J. (Ed.), Heavy Metals in Soils. , 3rd ed. Springer Science+Business Media, Dordrecht, pp. 335–365.
Wang, Y.-Y., Hsieh, T.-E., 2007. Effect of UV curing on electrical properties of a UV-curable co-polyacrylate/silica nanocomposite as a transparent encapsulation resin for device packaging. Macromol. Chem. Phys. 208, 2396–2402.
Weng, Y.-X., Jin, Y.-J., Meng, Q.-Y., Meng, L., Zhang, M., Wang, Y.-Z., 2013. Biodegradation behavior of poly(butylene adipate-co-terephthalate) (PBAT), poly(lactic acid) (PLA), and their blend under soil conditions. Polym. Test. 32, 918–926.